ACS OMEGA

http://pubs.acs.org/journal/acsodf

Article

Expanding the SiMPl Plasmid Toolbox for Use with Spectinomycin/Streptomycin

Navaneethan Palanisamy,* Jara Ballestin Ballestin, and Barbara Di Ventura*

Cite This: *ACS Omega* 2021, 6, 14148−14153

Read Online

ACCESS | Metrics & More | Article Recommendations | Supporting Information

ABSTRACT: We recently developed the SiMPl plasmid toolbox, which is constituted by pairs of plasmids, generically indicated as pSiMPl^{x}_N and pSiMPl^{x}_C, which can be stably maintained in *Escherichia coli* with a single antibiotic x. The method exploits the split intein gp41−1 to reconstitute the enzyme conferring resistance toward the antibiotic x, whereby each enzyme fragment is expressed from one of the plasmids in the pair. pSiMPl plasmids are currently available for use with ampicillin, kanamycin, chloramphenicol, hygromycin, and puromycin. Here, we introduce another pair for use with spectinomycin/streptomycin, broadening the application spectrum of the SiMPl toolbox. To find functional splice sites in aminoglycoside adenylyltransferase, we apply a streamlined strategy looking exclusively at the flexibility of native cysteine and serine residues, which we first validated splitting the enzymes conferring resistance toward ampicillin, kanamycin, chloramphenicol, and hygromycin. This strategy could be used in the future to split other enzymes conferring resistance toward antibiotics.

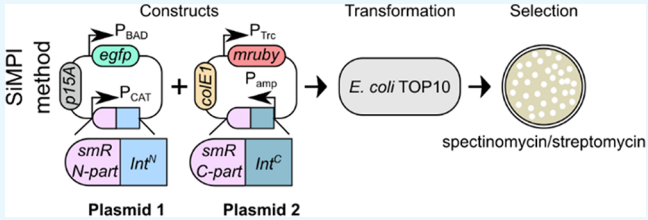

INTRODUCTION

We have recently devised a method based on split intein-mediated enzyme reconstitution that allows selecting bacterial and mammalian cells containing two plasmids with a single antibiotic, which we named SiMPl.[1] Inteins are proteins that excise themselves out of host proteins in an autocatalytic reaction that results in a peptide bond joining the polypeptides originally flanking the intein.[2,3] Split inteins are constituted by two separate fragments that need to associate to reconstitute a functional intein. Therefore, during the process of splicing, split inteins make fusions between two previously independent proteins or peptides. The SiMPl method consists in splitting the enzyme conferring resistance toward the antibiotic of choice—here indicated as x—in an N- and a C-terminal fragment, each *per se* dysfunctional. The coding sequence of the N-terminal fragment of the enzyme is fused to the coding sequence of the N-terminal fragment of the gp41−1 split intein[4] and is cloned in one plasmid in place of the full-length resistance gene, giving rise to the pSiMPl^{x}_N plasmid. The coding sequence of the C-terminal fragment of the enzyme is likewise fused to the coding sequence of the C-terminal fragment of gp41−1 and is cloned in another plasmid, giving rise to the pSiMPl^{x}_C plasmid. The pSiMPl^{x}_N and pSiMPl^{x}_C plasmid pair for use in bacteria is characterized by compatible origins of replication and can be co-transformed into competent bacterial cells. Those cells that pick both plasmids up following the transformation procedure survive in the presence of the antibiotic x because the full-length enzyme that confirms resistance toward x gets reconstituted inside them. Thus, these cells are able to form colonies on the selection plate. SiMPl is, as the same says, extremely simple in concept and usage. The challenge consisted in identifying functional splice sites in the enzymes conferring resistance toward the antibiotics. To this end, we applied a rational strategy consisting in looking at (i) the flexibility of the amino acids, using the coarse-grained CABS-flex protein structure flexibility simulation tool[5] that calculates the fluctuations of the Cα atoms (root-mean-square fluctuation or RMSF) of the protein backbone structural ensemble, (ii) their conservation, (iii) their surface accessibility, and (iv) their location relative to the active site.[1] We considered all these features because, to ensure high splicing efficiency, we decided to insert in the enzymes, beyond the catalytic serine, five additional amino acids, called local exteins (SGYSS), which are residues found in the natural context of gp41−1.[4] However, when looking for additional splice sites in puromycin acetyltransferase (PAT) that would give rise to differently sized enzyme fragments, we realized that identifying highly flexible native serines or cysteines also led to functional splice sites.[1] The local exteins appeared not to be necessary, and gp41−1 was able to splice itself out and reconnect the flanking enzyme fragments using either serine or cysteine as catalytic residues to a degree compatible with the growth of the double transformants in the presence of puromycin. Scarless reconstitution has the

Received: February 4, 2021
Accepted: April 26, 2021
Published: May 21, 2021

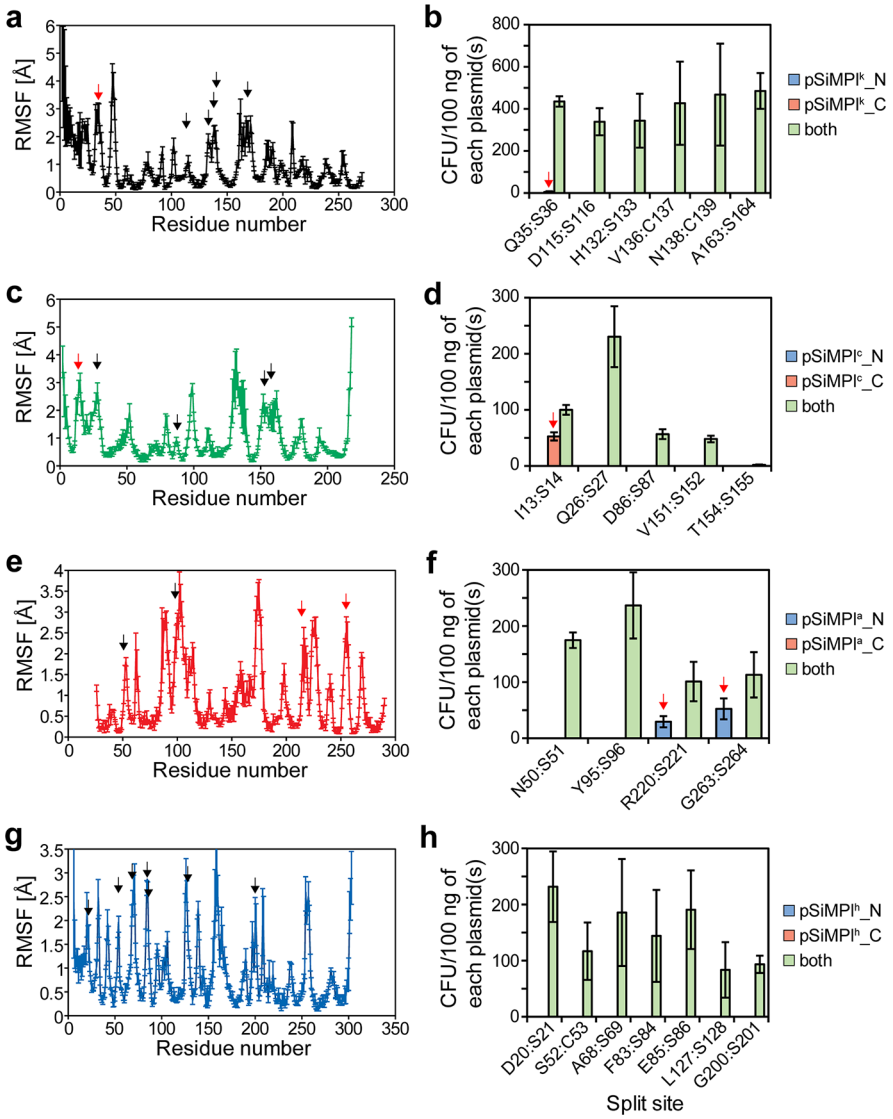

Figure 1. Identification of splice sites in enzymes conferring resistance toward antibiotics using a streamlined computational strategy. (a, c, e, g) Root-mean-square fluctuation (RMSF) of Cα atoms in aminoglycoside 3′-phosphotransferase (PDB ID: 4ej7; a), chloramphenicol acetyltransferase (PDB ID: 1q23; c), TEM-1 β-lactamase (PDB ID: 1zg4; e), and hygromycin B phosphotransferase (PDB ID: 3w0s; g) obtained by submitting the crystal structures to the CABS-flex 2.0 webserver.[5] Values represent mean ± S.E.M. of three independent simulations with different seed values. Black arrow, functional splice site. Red arrow, splice site corresponding to one of the two enzyme fragments having activity. (b, d, f, h) Bar graphs showing the transformation efficiency of the indicated SiMPl plasmids in chemically competent *E. coli* TOP10 cells grown on kanamycin (b), chloramphenicol (d), ampicillin (f), and hygromycin (h) selective plates after Gibson Assembly. Values represent mean ± S.E.M. of three independent experiments. Red arrow, splice site corresponding to one of the two enzyme fragments having activity.

advantage that the activity of the reconstituted enzyme is most likely the same as that of the full-length, native enzyme. Here, we wished to assess whether this streamlined strategy looking exclusively at the flexibility of native serines and cysteines could be generally applied to enzymes conferring resistance toward antibiotics. We first validate the method identifying many new functional splice sites for the enzymes conferring resistance toward ampicillin, kanamycin, chloramphenicol, and hygromycin. Then, using this strategy, we find functional splice sites for aminoglycoside adenylyltransferase and establish a novel SiMPl plasmid pair (pSiMPl^{s}) for use with spectinomycin/streptomycin.

RESULTS AND DISCUSSION

To validate whether a streamlined strategy, whereby only the flexibility of native serines and cysteines is considered, would lead to the prediction of functional splice sites on enzymes conferring resistance toward antibiotics, we first considered the same enzymes that we previously split: aminoglycoside 3′-phosphotransferase, the enzyme conferring resistance toward kanamycin (for simplicity, in the following referred to as APT); chloramphenicol acetyltransferase, the enzyme conferring resistance toward chloramphenicol (in the following referred to as CAT); TEM-1 beta-lactamase, the enzyme conferring resistance toward ampicillin (in the following referred to as TEM-1 β-L); and hygromycin B phosphotransferase, the enzyme conferring resistance toward hygromycin (in the following referred to as HPT). For all these enzymes, the crystal structure is available. Using CABS-flex,[5] we calculated the flexibility of the Cα of each amino acid (given as RMSF) and took the serines and cysteines for which the RMSF was highest (Figure 1a,c,e,g). We predicted six, five,

https://doi.org/10.1021/acsomega.1c00649
ACS Omega 2021, 6, 14148−14153

four, and seven splice sites for APT, CAT, TEM-1 β-L, and HPT, respectively (Figure 1a,c,e,g). We cloned the corresponding N- and C-terminal fragments of each enzyme in the previously constructed pSiMPl_N/C plasmid pairs, respectively (Figure S1), and then transformed them either individually or together in *Escherichia coli* TOP10 cells. pSiMPl_N plasmids carry the *egfp* gene cloned in the multiple cloning site, while the pSiMPl_C ones carry the *mruby3* gene. For most predicted splice sites, we obtained colonies only when co-transforming both pSiMPl plasmids (Figure 1b,d,f,h and Figure S2). One of the six predicted splice sites for APT (Q35:S36) and one of the five predicted splice sites for CAT (I13:S14) resulted in the C-terminal fragment of the enzymes having some level of activity (Figure 1b,d). Similarly, for TEM-1 β-L, splice sites R220:S221 and G263:S264 resulted in N-terminal fragments having some activity (Figure 1f). When using information solely on structure flexibility, it is indeed impossible to computationally predict whether the fragments will have activity on their own or not. However, it is easy to experimentally identify such cases and exclude them afterward. Recently, Ho and colleagues proposed an empirical method to identify functional splice sites on proteins of interest called intein-assisted bisection mapping (IBM).[6] With this method, the authors predicted two hotspots for splice sites in TEM-1 β-L; splice site G263:S264 predicted by our computational method lies in the second hotspot identified by IBM.[6] However, our experimental results showed that the N-terminal fragment of the enzyme split at this position has some activity, and thus we would not consider this a functional site. Likewise, Jillette and colleagues applied a purely experimental pipeline based on trial-and-error and successfully identified eight splice sites for HPT[7] (tested in mammalian cells), among which three were found by our rational approach as well. This indicates that several strategies exist to find functional splice sites in enzymes conferring resistance toward antibiotics. We note that ours, a purely computational method, is less cumbersome than any other purely experimental one, as it restricts the numbers of samples to test beforehand.

All splice sites found to be functional were surface-exposed (Figures S3 and S4), suggesting that high flexibility largely reflects accessibility as well. Agarose gel electrophoretic analysis of the plasmid DNA extracted from a randomly picked colony indicated the presence of both pSiMPl plasmids for all antibiotics tested (Figure S5). Moreover, polymerase chain reaction (PCR) confirmed the presence of the genes of interest (*egfp* and *mruby3*) (Figures S6 and S7) and the absence of an intact resistance gene (Figure S8). We also verified by Western blot that protein splicing occurred in all cases (Figures S9−S12). Stable maintenance of pSiMPl plasmids in *E. coli* cells was verified by growing bacterial cultures with the respective antibiotics for 14 days and taking samples every 7 days to extract plasmid DNA (Figure S13).

Next, we characterized the different splice sites in terms of bacterial growth and transformation efficiency. *E. coli* TOP10 cells were transformed with all pSiMPl plasmid pairs corresponding to the different splice sites of the various enzymes, and cultures were grown in 96-well microtiter plates in nutrient broth with the appropriate antibiotics (Figure S14a−d). All splice sites supported bacterial growth in liquid culture to a similar extent, with few exceptions showing a longer lag phase (splice site T154:S155 for CAT and splice sites F83:S84 and L127:S128 for HPT). This was also reflected in the generation time, which was similar for most constructs (Figure S14e). Since TEM-1 β-L also confers resistance toward carbenicillin (a variant of ampicillin; Figure S15a,b), we tested the two newly identified splice sites as well as the one previously identified (S104:P105[1]) with this antibiotic and found that they all supported bacterial growth to the same extent as in the presence of ampicillin (Figure S15d−f). As positive control, we took the full-length enzyme encoded on pTrc99a (Figure S15c). The generation time for bacteria expressing the newly identified split enzyme variants was indistinguishable for media containing ampicillin and carbenicillin (Figure S15g). The transformation efficiency for the pSiMPl pairs for usage with kanamycin, chloramphenicol, and ampicillin was equivalent to that of conventional, full-length enzyme-bearing plasmids only at high total plasmid concentration (100 ng; Figure S16). At lower total plasmid concentrations (1 and 0.1 ng), on the other hand, the transformation efficiencies significantly decreased and varied between the different constructs (Figure S16). It is to be noted, though, that we are comparing transformation of the pSiMPl pairs to transformation of single plasmids.

We previously observed the spontaneous appearance of a mutation within reconstituted HPT split at E255:L256, which was likely necessary for the function of the enzyme.[1] Interestingly, also for some of the new split versions of HPT, a mutation within the N-terminal fragment was acquired (Figure S17a). In some cases, instead of a mutation within the coding sequence, an insertion within the promoter arose (Figure S17b). We speculate that these mutations have the effect of increasing the enzyme activity and expression level, respectively, and thus bacteria carrying them would have an advantage over the other ones. We indirectly tested this hypothesis by comparing the growth curves and generation times of bacteria carrying either wild-type HPT, HPT^{T9R}, or the construct with the mutated promoter. The advantage of the mutations was particularly evident through the generation time, which was shorter for both mutations than for the wild type (Figure S17c,d).

Finally, we checked whether the streamlined strategy could be applied with another split intein, namely, *Npu* DnaE, which has cysteine as catalytic residue.[8] We took the splice sites that we already identified when using gp41−1 in correspondence to native cysteines—namely, V136:C137 and N138:C139 in APT and S52:C53 in HPT—and tested if they supported bacterial growth when *Npu* DnaE was used instead of gp41−1. We obtained colonies only for splice site V136:C137 in APT. The splice site in HPT gave also rise to colonies. While for the APT construct based on the splice site V136:C137 there was no difference between *Npu* DnaE- or gp41−1-mediated enzyme reconstitution in terms of growth in liquid medium (Figure S18a,b), for the HPT construct based on splice site S52:C53 bacterial growth was better with gp41−1 than *Npu* DnaE (Figure S18c,d). These data suggest the efficiency of splicing and, consequently, the amount of reconstituted HPT to be higher when using gp41−1. This is interesting and at first counterintuitive, considering that cysteine is the natural catalytic residue for *Npu* DnaE and not gp41−1. Nonetheless, gp41−1 is the fastest split intein known to date, and thus we speculate that the slightly suboptimal splicing due to the presence of the cysteine instead of the serine at the catalytic site results nonetheless in more efficient splicing than the one achieved by *Npu* DnaE.

After validating the streamlined strategy to locate splice sites using APT, CAT, TEM-1 β-L, and HPT, we proceeded with its

https://doi.org/10.1021/acsomega.1c00649
ACS Omega 2021, 6, 14148−14153

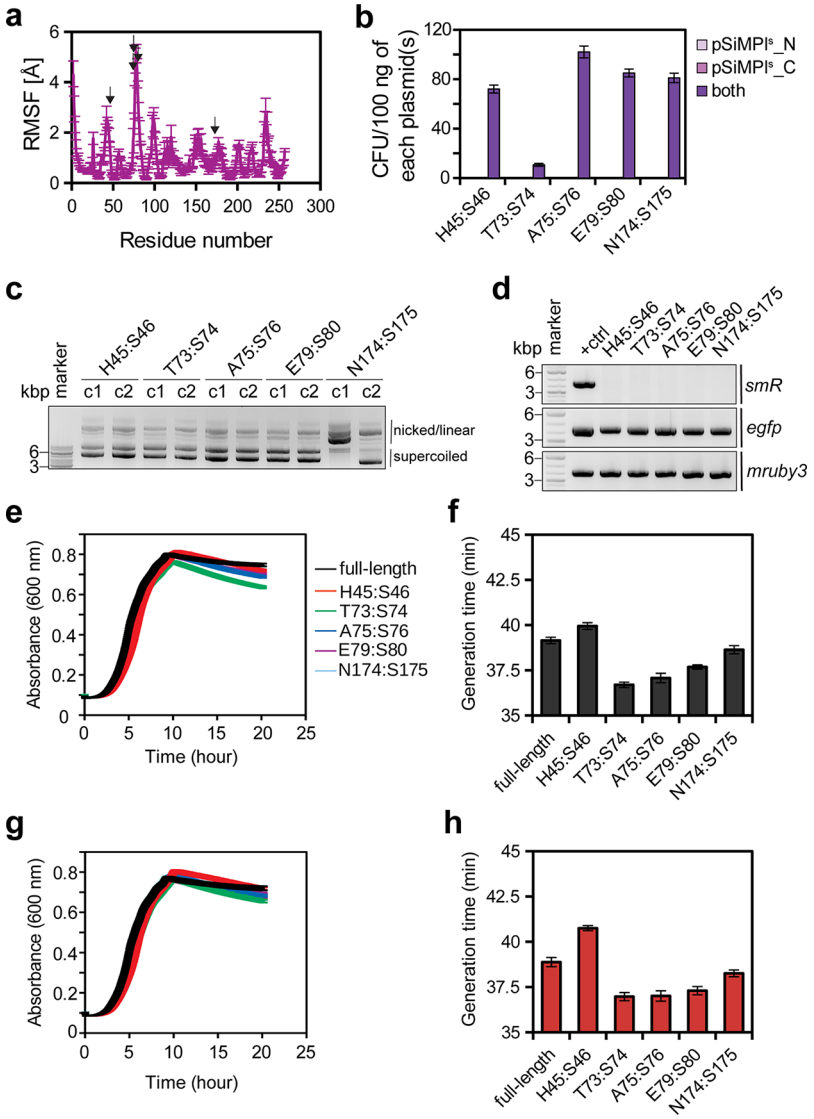

Figure 2. Identification of splice sites in aminoglycoside adenylyltransferase. (a) Root-mean-square fluctuation (RMSF) of Cα atoms in aminoglycoside adenylyltransferase obtained by submitting to the CABS-flex 2.0 webserver[5] the 3D model structure obtained by SWISS-MODEL[9] using the crystal structure of *S. enterica* AadA as the template (PDB ID: 5g4a). Values represent mean ± S.E.M. of three independent simulations with different seed values. Black arrow, functional splice site. (b) Bar graphs showing the transformation efficiency of the indicated plasmids in chemically competent *E. coli* TOP10 cells grown on spectinomycin after Gibson Assembly. Values represent mean ± S.E.M. of three independent experiments. (c) Ethidium bromide-stained agarose gel showing plasmid DNA isolated from a randomly picked clone obtained after transformation with the SiMPIs plasmids for selection on spectinomycin/streptomycin. (d) PCR analysis of the SiMPIs plasmids isolated from bacteria. pBAD33 into which the full-length *smR* resistance gene (derived from pCDF-1b) was cloned in place of *camR* was used as a control to show the product obtained after amplification of the full-length resistance gene. (e, g) Growth curves of *E. coli* TOP10 cells transformed with the pSiMPIs plasmids and grown in a 96-well plate in a medium containing spectinomycin (e) or streptomycin (g) measured every 2.4 min for 20 h in a plate reader. Experiments were performed twice (biological replicates) with technical triplicates each time. Values represent mean ± S.E.M. (f, h) Bar graphs showing the generation time for the growth curves shown in (e) and (g), respectively, calculated using the R package Growthcurver.[12]

application to aminoglycoside adenylyltransferase, the enzyme that confers resistance toward spectinomycin/streptomycin. First, we needed to model the 3D structure of the enzyme. We used the fully automated protein structure homology-modeling server SWISS-MODEL[9] with the crystal structure of *Salmonella enterica* AadA as the template (PDB ID: 5g4a). Using again CABS-flex[5] on the model structure, we calculated the flexibility of the Cα of each amino acid (given as RMSF) and identified five serines for which the RMSF was highest (Figure 2a). We then constructed pSiMPIs_N and pSiMPIs_C for all predicted splice sites and found them to be functional (Figure 2b). Splice site T73:S74 led to fewer colony forming units than the other sites. Interestingly, we noticed that splitting CAT at T154:S155 also led to fewer colonies compared to the other split versions. Whether splitting between a threonine and a serine is always problematic is worth future exploration. As before, we confirmed that the splice sites were surface-exposed (Figure S19) and that both pSiMPl plasmids were present in the bacteria (Figure 2c). PCR confirmed the presence of the *egfp* and *mruby3* genes and the absence of the full-length resistance gene (Figure 2d). Finally, we measured the growth curves of *E. coli* TOP10 cells transformed with all the pSiMPIs plasmid pairs on spectinomycin (Figure 2e) and streptomycin (Figure 2g).

https://doi.org/10.1021/acsomega.1c00649
ACS Omega 2021, 6, 14148−14153

Despite not being all identical, there were no major differences in the growth curves for the different splice sites. The generation times were also minimally lower for four out of the five constructs compared to the full-length enzyme for both antibiotics (Figure 2f,h).

Here, we presented a very simple strategy to identify splice sites in enzymes conferring resistance toward antibiotics, which led to a success rate of 100%. However, we believe that, despite being an important feature, structure flexibility alone would not suffice to find, within a generic protein of interest, splice sites corresponding to a sufficient activity with high success rates. Indeed, previously, structure flexibility was found not to be a good feature to predict functional splice sites in proteins.[10] A currently available computational method to predict split sites on any protein of interest indeed incorporates several other features beyond structure flexibility.[11] Nonetheless, this easy strategy seems to be well suited for the specific case in which the screening assay is connected to survival.

MATERIALS AND METHODS

Protein Cα Fluctuation Analysis. The X-ray structures of aminoglycoside 3′-phosphotransferase (PDB ID: 4ej7), chloramphenicol acetyltransferase (PDB ID: 1q23), TEM-1 β-lactamase (PDB ID: 1zg4), and hygromycin B phosphotransferase (PDB ID: 3w0s) were retrieved from the RCSB Protein Data Bank (https://www.rcsb.org/). The aminoglycoside adenylyltransferase structure was modeled on the SWISS-MODEL server[9] using the crystal structure of *S. enterica* AadA as a template (PDB ID: 5g4a) and SmR protein sequence from pCDF-1b as an input sequence. Cα fluctuation analysis was performed using the CABS-flex 2.0 webserver[5] with default parameters except for the seed value, which was changed in each independent coarse-grained simulation.

Plasmid Construction. The KanR$^{1-118}$ + SGY and SSS + KanR$^{119-271}$ regions from the previously constructed pSiMPl^{k}_N and pSiMPl^{k}_C plasmids[1] were removed by performing PCR separately using primer pairs Gib_SiMPl_BB1_FP and Gib_SiMPl_BB1_RP and Gib_SiMPl_BB2_FP and Gib_SiMPl_BB2_RP, respectively. The complete list of primers used in the present study is given in the Supporting Information. All PCR amplifications were performed with Phusion Flash High-Fidelity PCR Master Mix (2×) from ThermoScientific using a Biometra-Thermocycler from Analytik Jena. The N- and C-terminal fragments of the resistance genes were amplified separately using the appropriate primer pairs (Supporting Information). These primer pairs were designed to have overlapping sequences at the 5′ end with the respective plasmid backbones. Plasmids were finally assembled by Gibson Assembly. Chemically competent *E. coli* TOP10 cells (Invitrogen) were used for all cloning purposes. For selection, kanamycin, chloramphenicol, ampicillin, hygromycin, spectinomycin, and streptomycin were used at final concentrations 50, 35, 100, 100, 50, and 50 μg/mL, respectively. Plasmid isolation was performed using the Miniprep kit from Qiagen. Sanger sequencing of the plasmids was done at GATC (Eurofins Genomics).

Plasmid Stability Analysis. Bacterial cultures of *E. coli* TOP10 cells transformed with the SiMPl plasmids (pSiMPl^{k}, with APT split at D115:S116; pSiMPl^{c}, with CAT split at T154:S155; pSiMPl^{a}, with TEM-1 β-L split at N50:S51; pSiMPl^{h}, with HPT split at L127:S128; and pSiMPl^{s}, with aminoglycoside adenyltransferase split at T73:S74) were grown for an entire day at 37 °C with shaking. The following morning, the cultures were diluted 1000-fold in 4 mL of fresh nutrient broth containing the necessary antibiotics and were grown at 37 °C with shaking again the whole day. This procedure was repeated consecutively for 14 days. Samples were collected after 1, 7, and 14 day(s) for plasmid isolation. The presence of pSiMPl plasmids was verified *via* agarose gel electrophoresis and ethidium bromide staining.

Bacterial Growth Analysis. Bacterial growth curves were acquired on the BioTek Synergy H4 plate reader as previously described.[1] Briefly, overnight *E. coli* TOP10 cultures carrying the plasmids were diluted to a starting OD_{600} of 0.01 using fresh nutrient broth containing the necessary antibiotic. A total of 120 μL of the freshly diluted cultures was transferred into a flat-bottom 96-well plate. The plate was sealed with the lid using parafilm tape. The parameters set were as follows: temperature = 37 °C; run time = 20 h; read interval = 2 min and 43 s; wavelength = 600 nm; shake = slow; shake once every 130 s; read = absorbance end point; read speed = normal; delay = 100 ms. The plate reader was preheated to 37 °C before the start of the experiment. Bacterial generation time (doubling time) was calculated using Growthcurver.[12]

Bacterial Transformation Efficiency Analysis. A total of 50 μL of chemically competent *E. coli* TOP10 cells (Invitrogen) was transformed with each SiMPl plasmid pair. Transformations were carried out by the standard heat shock method and either 100, 10, 1, or 0.1 ng of total plasmid DNA concentration was used for the transformation. As single plasmid controls, pET28a empty plasmid was used for kanamycin, pBAD33-EGFP was used for chloramphenicol, and pTrc99a-mRuby3 was used for ampicillin. Colonies were counted manually.

Western Blot. Western blots with bacterial samples were performed as previously described.[1] Bacterial cultures were grown from OD_{600} = 0.1 until $OD_{600} \approx 1$ at 37 °C and 250 rpm, and 200 μL of each culture was centrifuged at 14800 rpm for 1 min. Pellets were resuspended in 10 μL of 4× Laemmli sample buffer (Bio-Rad), and cells were lysed by incubating them at 95 °C for 10 min. The samples were then loaded onto a 12% Mini-PROTEAN TGX precast protein gel (Bio-Rad) and ran for ∼1 h at 120 V with 1× TGS running buffer. Proteins were transferred to PVDF membranes using Trans-Blot Turbo Transfer Packs and a Trans-Blot Turbo Transfer System (Bio-Rad) as per the manufacturer's protocol. After the transfer, membranes were first incubated with 4−5% BSA dissolved in TBST with shaking for 2 h at room temperature and rinsed with TBST. Then, the membranes were incubated with either rat anti-HA (1:2000, Cat# 11867423001, Sigma), or rabbit anti-FLAG (1:2000, Cat# AHP1074, Bio-Rad), or mouse anti-GAPDH (1:1000, Cat# G13-61 M, SignalChem) primary antibody at room temperature for 2 h. Following three times washing (each time lasting for 5 min) with TBST, membranes were incubated with either AlexaFluor 488-conjugated anti-rat (1:2000, Cat# A-11006, Invitrogen), or Cyanine5-conjugated anti-rabbit (1:2000, Cat# A10523, Invitrogen), or AlexaFluor 790-conjugated anti-mouse (1:2000, Cat# A28182, Invitrogen) secondary antibody at room temperature for 1 h. Unbound secondary antibodies were removed by washing the membrane twice with TBST (each time lasting for 5 min). Fluorescence signals were measured with an Amersham Typhoon imaging system (GE Healthcare) using 488, 635, and 785 nm wavelength lasers.

https://doi.org/10.1021/acsomega.1c00649
ACS Omega 2021, 6, 14148−14153

■ ASSOCIATED CONTENT

Supporting Information

The Supporting Information is available free of charge at https://pubs.acs.org/doi/10.1021/acsomega.1c00649.

Supplementary figures containing schematics of SiMPl plasmids; chloramphenicol acetyltransferase split at T154:S155; surface-accessibility of identified splice sites; agarose gel electrophoretic analysis for the presence of both the plasmids in *E. coli* cells; PCR results for the presence of both *egfp* and *mruby3* genes, and absence of intact resistance gene; Western blot results; stable maintenance of pSiMPl plasmids in *E. coli* cells; characterization of the different splice sites in terms of bacterial growth and transformation efficiency; mutations in the HPT constructs; and construction of pSiMPl plasmids with different split inteins, and list of primers used in this study (PDF)

■ AUTHOR INFORMATION

Corresponding Authors

Navaneethan Palanisamy − *Signalling Research Centres BIOSS and CIBSS, University of Freiburg, 79104 Freiburg, Germany; Institute of Biology II, Faculty of Biology, University of Freiburg, 79104 Freiburg, Germany;* Present Address: Chester Medical School, University of Chester, Bache Hall, Countess View, Chester, Cheshire CH2 1BR, United Kingdom.; orcid.org/0000-0003-0369-2316; Email: n.palanisamy@chester.ac.uk, navaneethan.palanisamy@biologie.uni-freiburg.de

Barbara Di Ventura − *Signalling Research Centres BIOSS and CIBSS, University of Freiburg, 79104 Freiburg, Germany; Institute of Biology II, Faculty of Biology, University of Freiburg, 79104 Freiburg, Germany*; Email: barbara.diventura@biologie.uni-freiburg.de

Author

Jara Ballestin Ballestin − *Signalling Research Centres BIOSS and CIBSS, University of Freiburg, 79104 Freiburg, Germany; Institute of Biology II, Faculty of Biology, University of Freiburg, 79104 Freiburg, Germany;* Present Address: ViraTherapeutics GmbH, Bundesstraße 27, 6063 Rum, Austria.

Complete contact information is available at: https://pubs.acs.org/10.1021/acsomega.1c00649

Author Contributions

N.P. conceived the study and performed computational analyses and all cloning and bacterial experiments. J.B.B. performed Western blotting. B.D.V. supervised the work, secured funding, and wrote the manuscript with input from N.P. and J.B.B.

Notes

The authors declare no competing financial interest.

The pSiMPl[s] plasmids (A75:S76) are deposited on Addgene (ID: 167203).

■ ACKNOWLEDGMENTS

We thank Mehmet Ali Öztürk for discussions and critical reading of the manuscript. This work was funded by the Deutsche Forschungsgemeinschaft (DFG) under Germany's Excellence Strategy through EXC294 (BIOSS—Center for Biological Signalling Studies) and EXC2189 (CIBSS—Centre for Integrative Biological Signalling Studies, Project ID 390939984).

■ REFERENCES

(1) Palanisamy, N.; Degen, A.; Morath, A.; Ballestin Ballestin, J.; Juraske, C.; Öztürk, M. A.; Sprenger, G. A.; Youn, J.-W.; Schamel, W. W.; Di Ventura, B. Split intein-mediated selection of cells containing two plasmids using a single antibiotic. *Nat. Commun.* **2019**, *10*, 4967.

(2) Di Ventura, B.; Mootz, H. D. Switchable inteins for conditional protein splicing. *Biol. Chem.* **2019**, *400*, 467−475.

(3) Shah, N. H.; Muir, T. W. Inteins: Nature's Gift to Protein Chemists. *Chem. Sci.* **2014**, *5*, 446−461.

(4) Carvajal-Vallejos, P.; Pallissé, R.; Mootz, H. D.; Schmidt, S. R. Unprecedented rates and efficiencies revealed for new natural split inteins from metagenomic sources. *J. Biol. Chem.* **2012**, *287*, 28686−28696.

(5) Kuriata, A.; Gierut, A. M.; Oleniecki, T.; Ciemny, M. P.; Kolinski, A.; Kurcinski, M.; Kmiecik, S. CABS-flex 2.0: a web server for fast simulations of flexibility of protein structures. *Nucleic Acids Res.* **2018**, *46*, W338−W343.

(6) Ho, T. Y. H.; Shao, A.; Lu, Z.; Savilahti, H.; Menolascina, F.; Wang, L.; Dalchau, N.; Wang, B. Intein-assisted bisection mapping systematically splits proteins for Boolean logic and inducibility engineering. *bioRxiv* **2020**, DOI: 10.1101/2020.11.30.381921.

(7) Jillette, N.; Du, M.; Zhu, J. J.; Cardoz, P.; Cheng, A. W. Split selectable markers. *Nat. Commun.* **2019**, *10*, 4968.

(8) Zettler, J.; Schütz, V.; Mootz, H. D. The naturally split Npu DnaE intein exhibits an extraordinarily high rate in the protein trans-splicing reaction. *FEBS Lett.* **2009**, *583*, 909−914.

(9) Waterhouse, A.; Bertoni, M.; Bienert, S.; Studer, G.; Tauriello, G.; Gumienny, R.; Heer, F. T.; de Beer, T. A. P.; Rempfer, C.; Bordoli, L.; Lepore, R.; Schwede, T. SWISS-MODEL: homology modelling of protein structures and complexes. *Nucleic Acids Res.* **2018**, *46*, W296−W303.

(10) Apgar, J.; Ross, M.; Zuo, X.; Dohle, S.; Sturtevant, D.; Shen, B.; de la Vega, H.; Lessard, P.; Lazar, G.; Raab, R. M. A predictive model of intein insertion site for use in the engineering of molecular switches. *PLoS One* **2012**, *7*, No. e37355.

(11) Dagliyan, O.; Krokhotin, A.; Ozkan-Dagliyan, I.; Deiters, A.; Der, C. J.; Hahn, K. M.; Dokholyan, N. V. Computational design of chemogenetic and optogenetic split proteins. *Nat. Commun.* **2018**, *9*, 4042.

(12) Sprouffske, K.; Wagner, A. Growthcurver: an R package for obtaining interpretable metrics from microbial growth curves. *BMC Bioinf.* **2016**, *17*, 172.